NeuroImage 59 (2012) 1997–2006

Contents lists available at SciVerse ScienceDirect

NeuroImage

journal homepage: www.elsevier.com/locate/ynimg

Neurovascular coupling is brain region-dependent

Ian M. Devonshire [1,3], Nikos G. Papadakis [2,3], Michael Port, Jason Berwick, Aneurin J. Kennerley, John E.W. Mayhew, Paul G. Overton *

Department of Psychology, University of Sheffield, Western Bank, Sheffield, S10 2TN, United Kingdom

ARTICLE INFO

Article history:
Received 25 March 2011
Revised 15 September 2011
Accepted 19 September 2011
Available online 29 September 2011

ABSTRACT

Despite recent advances in alternative brain imaging technologies, functional magnetic resonance imaging (fMRI) remains the workhorse for both medical diagnosis and primary research. Indeed, the number of research articles that utilise fMRI have continued to rise unabated since its conception in 1991, despite the limitation that recorded signals originate from the cerebral vasculature rather than neural tissue. Consequently, understanding the relationship between brain activity and the resultant changes in metabolism and blood flow (neurovascular coupling) remains a vital area of research. In the past, technical constraints have restricted investigations of neurovascular coupling to cortical sites and have led to the assumption that coupling in non-cortical structures is the same as in the cortex, despite the lack of any evidence. The current study investigated neurovascular coupling in the rat using whole-brain blood oxygenation level-dependent (BOLD) fMRI and multi-channel electrophysiological recordings and measured the response to a sensory stimulus as it proceeded through brainstem, thalamic and cortical processing sites — the so-called whisker-to-barrel pathway. We found marked regional differences in the amplitude of BOLD activation in the pathway and non-linear neurovascular coupling relationships in non-cortical sites. The findings have important implications for studies that use functional brain imaging to investigate sub-cortical function and caution against the use of simple, linear mapping of imaging signals onto neural activity.

Introduction

Functional magnetic resonance imaging (fMRI) is a key methodology employed by modern neuroscientific research in order to characterise fundamental aspects of human brain function and their changes in health and disease (Moonen and Bandettini, 2000). However, the technique maps brain activity indirectly by measuring activity-induced haemodynamic changes. Since we are ultimately interested in the brain's neural activity, an understanding of neurovascular coupling, the relationship linking the measured haemodynamic responses to neural activity, is essential for the interpretation and practical exploitation of fMRI (Lauritzen and Gold, 2003; Logothetis and Wandell, 2004).

However, although it is acknowledged that neurovascular coupling probably varies even between areas with similar neuronal populations (Huettel et al., 2004; Logothetis and Wandell, 2004), human fMRI studies routinely compare responses across the brain with the *implicit* assumption that coupling is spatially invariant. This assumption has been largely forced upon the imaging community because coupling has thus far only been studied in detail in cortical areas (Lauritzen and Gold, 2003; Logothetis and Wandell, 2004; Martuzzi et al., 2009) which has prompted calls for its urgent study in non-cortical areas (Ances et al., 2008; Ekstrom, 2010). To exemplify a potential problem, if sensory stimuli differentially activate cortical and subcortical auditory structures, as has been demonstrated with fMRI (Sigalovsky and Melcher, 2006), it is impossible to infer differential levels of neural activation in the contributing structures without an understanding of neurovascular coupling at cortical and subcortical sites. It is even possible that particular vascularisation patterns may prevent, or even reverse, the BOLD response (Boorman et al., 2010; Ekstrom, 2010).

Neurovascular coupling can be affected not only by the intrinsic characteristics of the vascular beds in different regions, but also by differences in the functional processes that link neural activity, via changes in metabolism, to alterations in local cerebral blood flow (CBF). Cortical and subcortical sites differ on both counts. The pattern of vascular innervation, capillary density, as well as the diameter of feeding arteries in relation to their peripheral branches all differ between cortical and subcortical sites (Cavaglia et al., 2001; Duvernoy et al., 1981; Gobel et al., 1990; Rieke, 1987). The magnitude of BOLD signals also crucially depend on the ratio of fractional changes in CBF to the local cerebral metabolic rate of oxygen consumption ($CMRO_2$), a ratio that varies throughout the brain (Ances et al., 2008; Chiarelli et al., 2007; Tuunanen et al., 2006; Vafaee and Gjedde, 2004); differences

* Corresponding author. Fax: +44 114 276 6515.
E-mail address: p.g.overton@sheffield.ac.uk (P.G. Overton).
[1] Present address: School of Biomedical Sciences, The Medical School, Queen's Medical Centre, University of Nottingham, Nottingham, NG7 2UH, United Kingdom.
[2] Present address: Iatropolis-Magnetic Tomography SA, Ethnikis Antistaseos 54–56, Athens 152 31, Greece.
[3] These authors contributed equally to the work.

1053-8119/$ – see front matter © 2011 Elsevier Inc. All rights reserved.
doi:10.1016/j.neuroimage.2011.09.050

in local vascular patterns are highly likely to contribute to the variability of this ratio. Furthermore, the functional coupling process in the cortex appears to differ from that in the brainstem, in that cortical coupling involves neuronal nitric oxide (Cholet et al., 1997; Gotoh et al., 2001), whereas brainstem coupling involves adenosine (Gotoh et al., 2001). These structural and functional differences between the cortex and subcortex make a compelling *a priori* case for assuming that neurovascular coupling will differ between different brain regions.

The current study examines coupling at various stations throughout the rat's whisker-to-barrel (WTB) pathway, both the anatomy and neural behaviour of which have been widely studied (Frostig, 2006; Petersen, 2007). The pathway elicits robust cortical responses, both neural and haemodynamic, which have been examined extensively by our group and others (Devonshire et al., 2004; Devor et al., 2003; Hewson-Stoate et al., 2005; Jones et al., 2004; Sheth et al., 2003), yet the characteristics of the haemodynamic responses elicited in sub-cortical structures is largely unknown. Our aim was to provide a substantial improvement in the interpretation and exploitation of functional neuroimaging data by conducting whole brain fMRI experiments in parallel with multi-electrode electrophysiology to study for the first time neurovascular coupling in subcortical areas and compare it to its cortical counterpart.

Materials and methods

Animal preparation

A total of 18 female Hooded Lister rats weighing between 220 and 320 g were used, after having been kept on a 12-h dark/light cycle at a temperature of 22 °C with food and water available *ad libitum*. Great care was taken to maintain consistency in surgical and experimental scheduling between the fMRI and electrophysiology animal groups. Animals were anaesthetised with chloral hydrate (0.14 g/kg i.p.) and urethane (1.1 g/kg i.p.), cannulated for mean arterial blood pressure (MABP) monitoring and intravenous infusions, tracheotomised and artificially ventilated. Phenylephrine (0.13–0.26 mg/h) was infused to maintain MABP between 100 and 110 mm Hg. Rectal temperature was maintained at 37 °C using a homeothermic blanket. Procedures were performed with Home Office approval under the Animals (Scientific Procedures) Act 1986.

Whisker stimulation

The entire whisker pad on the left of the rat's snout was stimulated electrically by inserting two stainless steel electrodes underneath the skin below whisker rows A and D. To modulate levels of evoked activity, we adopted a paradigm used in previous neurovascular coupling studies (Brinker et al., 1999; Detre et al., 1998; Ngai et al., 1999; Sheth et al., 2005; Ureshi et al., 2004): a square-wave current (1.6 mA; pulse-width 0.3 ms) was applied at a range of frequencies (1, 3, 5, 10, 15 and 20 Hz) for 40 s. Stimuli were presented in a block design with stimulation (40 s) and rest (140 s) conditions repeated six times at each frequency. An average response to each frequency was obtained and used in subsequent analysis for all measures. A shorter stimulation paradigm was used to visualise cortical activation during intrinsic imaging (see below).

fMRI

Previous studies of neurovascular coupling have been limited to the cortex largely because of technical constraints of the imaging methods used. Optical methods using visible wavelengths provide superficial (cortical) recordings only, due to the attenuation of light in deep tissue. Many animal fMRI studies use surface coils that have good signal sensitivity only around the cortex, where the coil is placed (Keilholz et al., 2004; Logothetis and Wandell, 2004). We have overcome the above limitations by using a high sensitivity *volume* coil, capable of whole brain fMRI.

A 3 T, 16 cm horizontal bore Magnex magnet (Magnex Scientific Ltd, UK) equipped with a Magnex 10 cm-id self-shielded gradient (10 kHz/mm max per axis), and an MRRS console was used (MRRS, Guildford, UK). A custom-built, quadrature, 8-strut birdcage coil (length: 40 mm, diameter: 35 mm) was used in transmit/receive mode. The open space between the coil's struts allowed free access to the rat's head, which was immobilised with a home-built Perspex stereotactic frame. BOLD imaging was performed over 12 × 2 mm-thick contiguous (but interleaved) coronal slices (Fig. 1) using fat-suppressed, single-shot, gradient-echo (GE) EPI with the following parameters: 64 × 64 image matrix, FOV = 3 × 3 cm, TE = 24 ms, TR = 2 s, flip angle = 90°. Anatomical images were acquired from 24 × 1 mm-thick contiguous coronal slices using a three-dimensional (3D) GE sequence with the following parameters: 128 × 128 image matrix, FOV = 3 × 3 cm, TE = 15 ms, TR = 250 ms, flip angle = 65°.

Data analysis

SPM2 (Functional Imaging Laboratory, Institute of Neurology, UCL; www.fil.ion.ucl.ac.uk/spm) was used for the analysis of fMRI data. First, the EPIs were realigned and spatially smoothed with a 3D Gaussian kernel (FWHM = 1.5 * voxel size). The paradigm was convolved with SPM's haemodynamic response function and high-pass filtered (cut-off at 2 * ISI = 360 s). SPM's MarsBar toolbox (http://marsbar.sourceforge.net) was used to extract time-series from 1.5 × 1.5 × 2 mm regions of interest from the relevant anatomical structure using the voxel with maximum statistical significance in response to the lowest stimulation frequency that produced robust responses: 5 Hz (cortex and thalamus) or 10 Hz (brainstem). Within each region of interest, all voxels were used for calculation of BOLD amplitudes. For illustration purposes, activation clusters are displayed with an uncorrected p-value threshold of 0.001 (family-wise error, FWE). For analytical purposes, the absolute BOLD data were summed between 0 and 40 s (ΣBOLD).

Intrinsic optical imaging

The precise cortical region into which the multi-channel electrode was to be inserted was selected using single-wavelength optical imaging, a procedure that can be used to obtain a two-dimensional activation map evoked by a sensory stimulus based upon changes in local haemodynamics of the tissue. The procedure has been described previously (Jones et al., 2001) and, as such, will only be briefly described here. The skull overlying the primary sensory cortex was thinned to translucency with a dental drill and the region illuminated with ~590 nm (orange) light. A digital camera (SMD1M60, Silicon Mountain

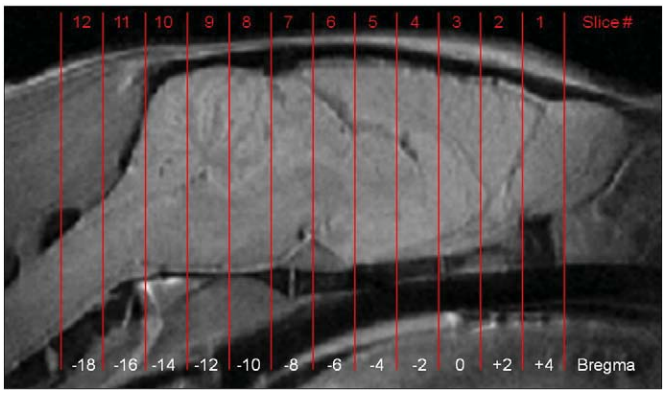

Fig. 1. Structural MRI scan in the sagittal plane showing the 12 × 2 mm-thick contiguous coronal slices acquired for functional scans. Distances from bregma are shown along the bottom edge.

Design Inc., USA; 15 Hz sampling frequency) was positioned directly above to record changes in light reflectance of the tissue which, at the wavelength chosen, predominantly represents changes in blood volume. The whiskers were electrically stimulated 30 times at 5 Hz for 1 s (inter-trial-interval = 25 s). The data were averaged over the 30 trials on a frame-by-frame basis and the changes in reflectance stored in grey-scale. The activation map was generated by removing noise components with principal-component analysis followed by a signal separation algorithm (Zheng et al., 2001).

Electrophysiology

The WTB pathway in the brain consists of 3 main stations: the trigeminal nuclei (primary sensory [PrV] and spinal [SpV], especially subnucleus interpolaris [SpVi]), thalamic nuclei (ventral posteromedial [VPM] and posterior [POm]) and somatosensory barrel cortex (S1) (Paxinos and Watson, 1998). Subcortical electrophysiological recording sites were matched to those sites from which robust and reliable BOLD fMRI responses could be elicited, i.e. SpVi and VPM. To record from SpVi, recording electrodes were inserted at an angle of 24° to the vertical, depth = 10 mm at the following co-ordinates: AP = −8.5 mm, ML = 2.9 mm. Electrodes were inserted into the VPM at co-ordinates: AP = −3.3 mm, ML = 2.4 mm, depth = 6 mm. Multi-channel silicon electrodes (NeuroNexus, Ann Arbor, MI, USA) were used for electrical recordings from all three brain regions. The electrodes were linear arrays of 16 channels (3 or 10 mm in overall length; 100 μm inter-site spacing, area of each site 177 μm^2, impedance 1.5 to 2.7 MΩ, probe width: 33 μm tip, 123 μm at uppermost electrode) and were positioned under microscopic control according to pre-defined haemodynamic activity (cortical site) or stereotactic co-ordinates (thalamus and brainstem sites).

Electrophysiological data from all trials were sampled 5 s before the first stimulus in the train for a total of 60 s and acquired at a sampling frequency of 6 kHz. The first ms after each stimulus pulse was removed to take account of the stimulus artefact; in all cases, the artefact was clearly identifiable and lasted no longer than 1 ms (verified by post-mortem recordings). Field potential recordings were generated by low-pass filtering the raw data (<300 Hz) combined with a 50 Hz notch filter, whereas MUA data were high-pass filtered (>500 Hz). To generate multi-unit spike counts for each stimulation frequency, the standard deviation of the 5 s pre-stimulus period was calculated for each electrode channel and each trial. The standard deviation values were averaged across all six trials for each channel and multiplied by 2.5 to serve as a spike-threshold. This threshold was used in order to detect the number of 'spikes' that occurred in the data in 1 ms bins. Spontaneous activity (calculated in the pre-stimulus period) was subtracted from the data in order to leave a pure measure of the stimulus-induced change in firing rate. Response profiles of sensory-evoked activation in the deep-brain relay stations have been previously characterised (Diamond et al., 1992; Khatri et al., 2004; Sosnik et al., 2001; Stewart and King, 1966; Temereanca and Simons, 2003) and these data (i.e. onset latency, duration and presence of sensory adaptation) were used in conjunction with MRI structural scans and histological verification of recording sites (see below) to identify activated channels within the electrode array, which were then averaged to generate a single time-series. The average of all individual responses presented at 1 Hz was then obtained and the maxima of this response used to normalise the data. To obtain measures comparable with fMRI responses, absolute LFP and MUA data were summed between 0 and 40 s (ΣLFP and ΣMUA respectively).

MRI and histological verification of recording sites

Upon completion of electrophysiological studies, recording sites were marked using a radio-frequency lesion generator at 5 mA for 240 s (RFG-4, Radionics, MA, USA (Brozoski et al., 2006)). The animals were perfused transcardially with saline followed by 4% paraformaldehyde and the brains removed. Recording sites were visualised by a combination of structural MRI scans and standard histological processing. For MRI measurements the brain was placed into a plastic container, filled with agar. This reduced air–tissue susceptibility artefacts around the cortex. The brain was scanned in a 7 T, 310 mm bore Bruker magnet (Bruker BioSpecAvance, MRI system B/C 70/30) fitted with an actively shielded micro imaging gradient set (Bruker BioSpin MRI GmbH B-GA12. 400 mT/m maximum strength per axis with 80 μs ramps). For RF transmission and reception we used a ^{1}H volume resonator (Bruker, 300 MHz, 1 kW max, outer diameter 118 mm/inner diameter 72 mm) and actively decoupled 20 mm (inner diameter) ^{1}H surface coil (Bruker 1P-T7399) respectively. We obtained high spatial resolution 3D-RARE scans (512*512*256 pixels, spatial resolution = 76 64*129 μm, RARE factor = 8, TR = 2000, TE = 15 ms, averages = 2) of the fixed brains before histological processing. A detailed procedure for histological processing using Nissl stains has been described previously (Zheng et al., 2001). To visualise the brainstem and thalamic recording sites, 50 μm sections from sagittal and coronal planes, respectively, were obtained and stained for Nissl substance using cresyl violet.

Results

Whole-brain fMRI

We used single-shot echo-planar imaging (EPI) in a 3 T MRI scanner to record BOLD responses to electrical whisker stimulation (1.6 mA) applied at frequencies between 1 and 20 Hz in anaesthetised rats. Stimuli were presented in a block design with stimulation periods (40 s) repeated every 180 s. The use of a custom-built bird-cage coil allowed us to collect data from 12×2 mm-thick contiguous coronal slices (Fig. 1); more than adequate to cover brainstem, thalamic and cortical stations of the WTB pathway. Of the major whisker-related subnuclei of the trigeminal complex, SpVi exhibited the most robust BOLD activation across the stimulation frequencies used. Likewise, thalamic BOLD activation was evoked most robustly in VPM (although notably more weakly than in the trigeminal complex or cortex). As a consequence, slices for BOLD analysis were standardised between animals to optimally correspond to SpVi (slice #10; Fig. 1), VPM (slice #5) and barrel cortex (slice #4). The three regions differed markedly in their responsiveness to stimulation at different frequencies (Figs. 2 and 3). While both the amplitude and integral of BOLD responses within the brainstem trigeminal nucleus increased monotonically with increasing stimulation frequencies, the thalamus only exhibited strong responses at or above 10 Hz, whereas BOLD responses in the cortex were greatest at mid-range stimulation frequencies (maximally at 5 Hz).

To the best of our knowledge this is the first time that BOLD activation has been evoked from sensory nuclei in the rodent brainstem using multi-frequency sensory stimulation (although see (Yu et al., 2005) for contrast-enhanced fMRI of brainstem activation), but the activation profiles are in line with what would be expected on the basis of the responsiveness of this area as demonstrated by previous electrophysiological recordings: brainstem sensory nuclei are known to reproduce incoming sensory stimuli with high fidelity (Sosnik et al., 2001) and would therefore be expected to exhibit greater BOLD responses with increasing stimulation frequency. The relatively weak BOLD activation that we observe in the thalamus is also in line with previous studies that have used sensory (Esaki et al., 2002; Zhao et al., 2008) and pharmacological (Mandeville et al., 2001) stimulation. Furthermore, BOLD activation in the thalamus can be entirely absent in response to sensory stimulation, despite strong activity in 'downstream' structures (Keilholz et al., 2004; Spenger et al., 2000). The frequency selectivity observed in the cortex can be explained using both functional and behavioural perspectives: rodents move

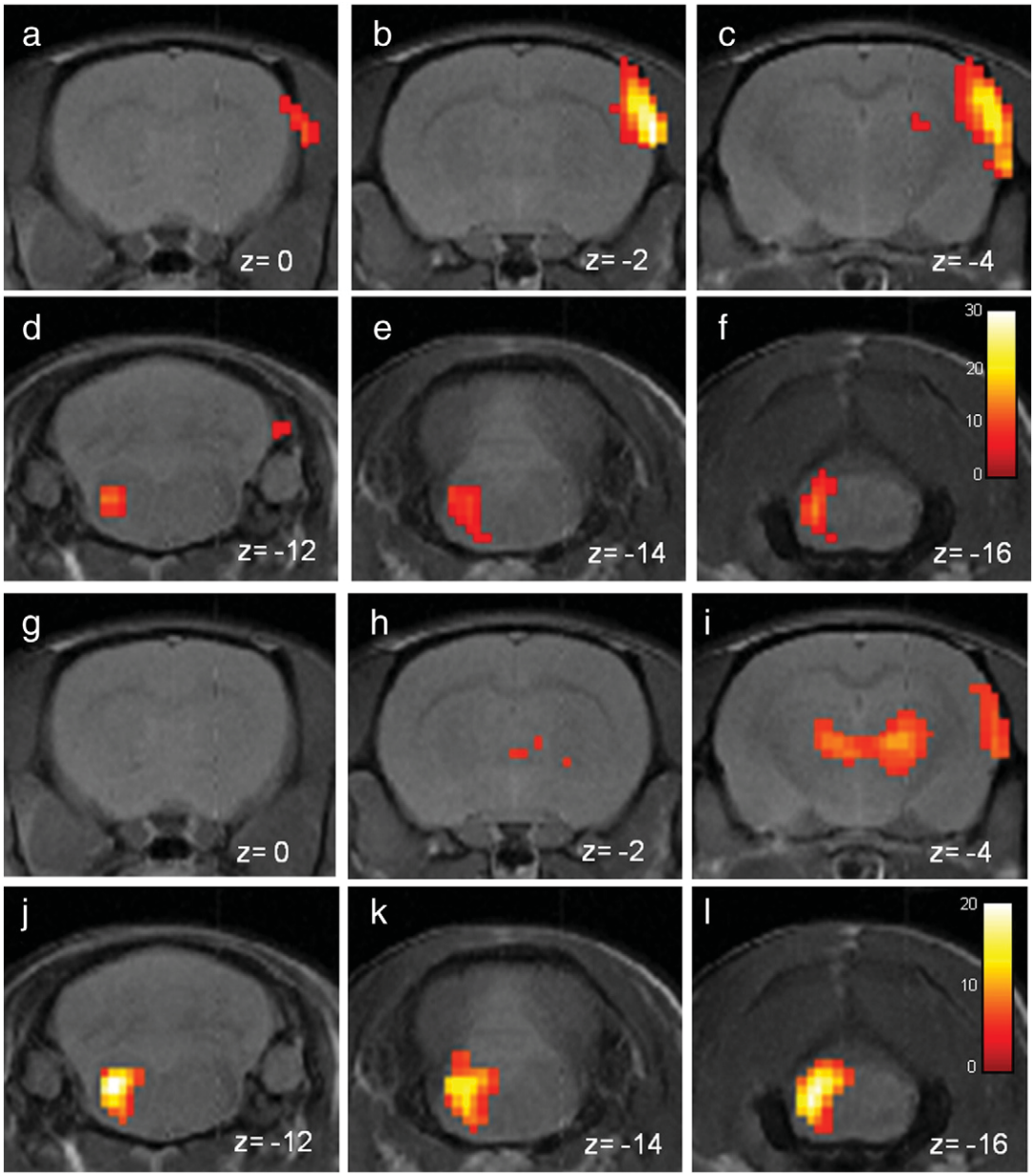

Fig. 2. BOLD fMRI activation maps in the coronal plane obtained in response to electrical stimuli presented at 5 Hz (upper panel; a–f) and 20 Hz (lower panel; g–l). The activation clusters are displayed with an uncorrected p-value threshold of 0.001 (family-wise error, FWE) and rendered onto high-resolution MRI anatomical images. Distance of the slice from bregma is shown in the lower-right corners.

their whiskers back and forth at specific frequencies when examining objects in their environment and this movement occurs in the range 5–12 Hz. Furthermore, the somatosensory cortex shows maximal integrated responsiveness at these frequencies (Hewson-Stoate et al., 2005; Keilholz et al., 2004; Sheth et al., 2003) and one would therefore expect greatest metabolic activity in this frequency range.

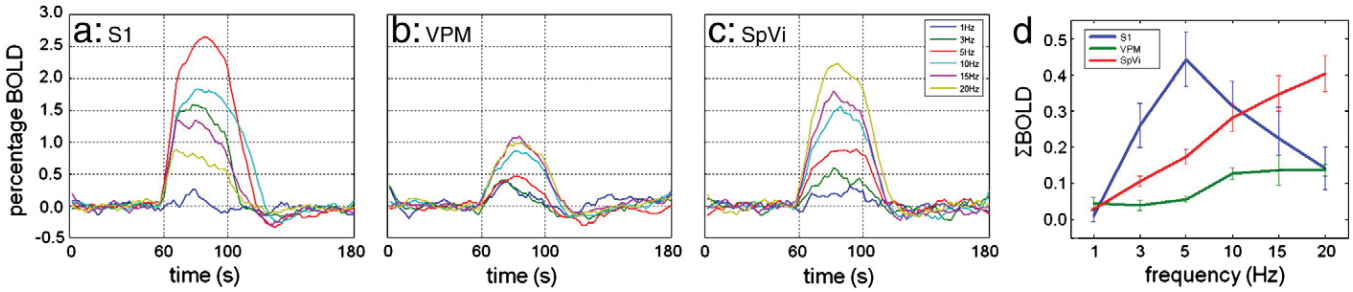

Fig. 3. Time series of BOLD fMRI responses to varying stimulation frequency in S1 (a), VPM (b) SpVi (c) and absolute $\sum$ of responses (d) during stimulus presentation (indicated by vertical dashed lines in a–c). Data are average responses from all animals.

Multi-site electrophysiology

In a parallel set of experiments, we recorded local field potentials (LFP) and multi-unit activity (MUA) from the same three stations of the WTB pathway (SpVi, VPM and barrel cortex) under identical experimental conditions. Correct placement of electrodes and successful recording of relevant nuclei was verified using a combination of histological processing, high-resolution MRI anatomical scanning (Fig. 4), intrinsic optical imaging (in the case of the cortex) and careful assessment of sensory-evoked response profiling (latency, duration and adaptation at high frequencies) based on previously published recordings (Diamond et al., 1992; Fraser et al., 2006; Minnery and Simons, 2003; Moreno et al., 2005; Shoykhet et al., 2000; Sosnik et al., 2001). Cortical electrodes were inserted to a depth of 1.5 mm.

In the current study, both LFP and MUA were recorded by differentially filtering the electrode recordings below 300 Hz and above 500 Hz, respectively. Average LFP and MUA responses as evoked by all stimulation frequencies are illustrated in Fig. 5 (i.e. the response represents the average response across all electrical pulses in a stimulus train in order to allow comparison between stimulation frequencies). As the sensory input travelled through the pathway, response latencies recorded in the three structures increased in a manner predicted by previous electrophysiology studies, with each structure exhibiting response profiles and stimulus adaptation rates that differed on account of their unique cytoarchitectonic make-up, intrinsic membrane properties and purported functional roles. In the trigeminal nucleus, the initial positive LFP waveform (Fig. 5g; peak latency: 2.15 ± 0.14 ms) and peak in MUA (Fig. 5c; peak latency: 2.95 ± 0.0 ms) signifies the first activity in the WTB pathway and these responses exhibit little adaptation with increasing stimulation frequency, in accordance with the role of the nucleus as a primary relay structure (Sosnik et al., 2001). Ascending projections then trigger a multi-component waveform in the thalamus (Fig. 5f; the first negative wave of which occurs after 4.27 ± 0.25 ms; Fig. 5b; MUA peak: 3.74 ± 0.78 ms) which displays greater adaptation than the response in the brainstem. In addition to projecting directly to the cortex, the thalamus is also responsible for sending a reciprocal connection back to the trigeminum which results in a negative LFP wave in the latter structure that only slowly returns to baseline (Fig. 5g; peak at 4.84 ± 0.19 ms) and, unlike the initial trigeminal response, exhibits a moderate level of adaptation resembling that observed in the structure of origin, the thalamus. The thalamocortical projection (Fig. 5e; LFP peak latency: 5.42 ± 1.82 ms; Fig. 5a MUA peak: 9.75 ± 2.17 ms) exhibits by far the greatest levels of adaptation, similar levels of which can also be observed in a reciprocal connection back to the thalamus (Figs. 5b,f).

Neurovascular coupling

In order to establish how well the underlying neural activity was predicted by the fMRI signal, the absolute ΣBOLD response (Fig. 3a)

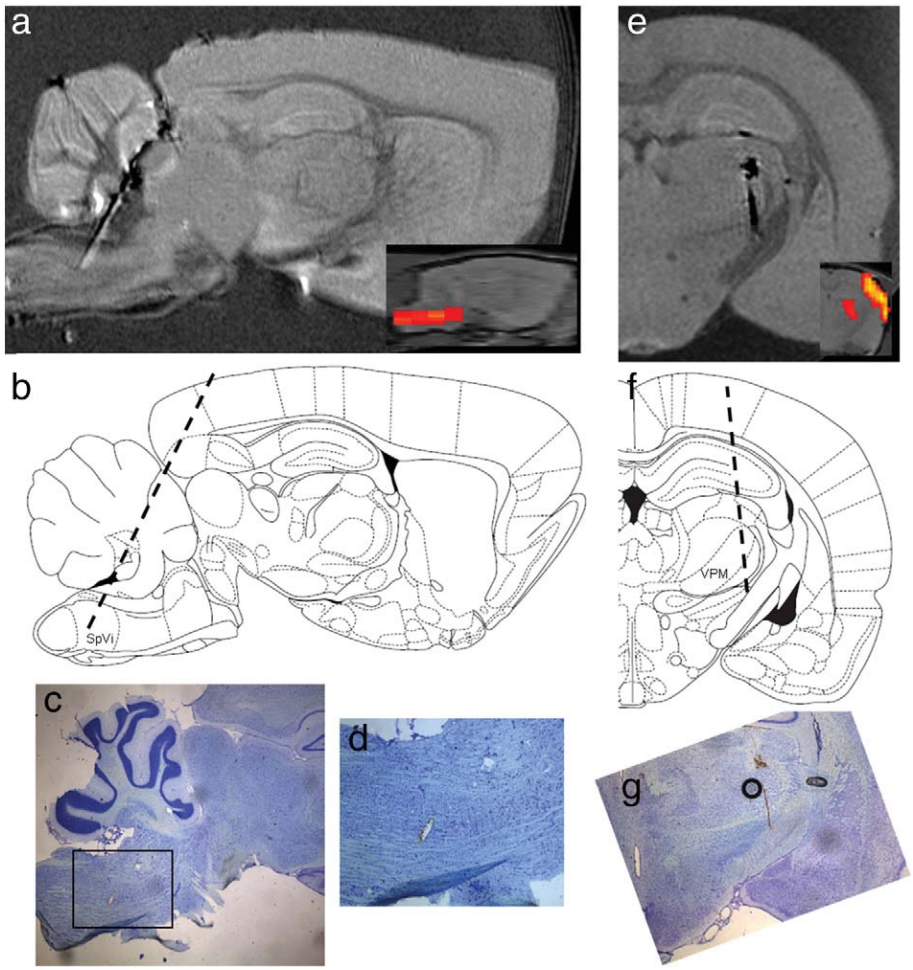

Fig. 4. Examples of MRI structural scans and results of histological processing to localise electrophysiology recording sites in SpVi (a–d) and VPM (e–g) nuclei. After the completion of an experiment, recording sites were lesioned and subsequently localised post-mortem by high-resolution structural MRI scans at 7 T (a, e) and stained for Nissl substance using cresyl violet (c, d, g). These are exemplified for a brainstem recording site (a–d) and thalamic site (e–g) alongside appropriate Paxinos and Watson (1998) atlas images which show the trajectory of the electrodes. Concordance of BOLD fMRI activation clusters and recording sites is illustrated with activation clusters (from separate animals) shown in insets in a and e. Air pocket artefacts near to midbrain structures (a) have been masked.

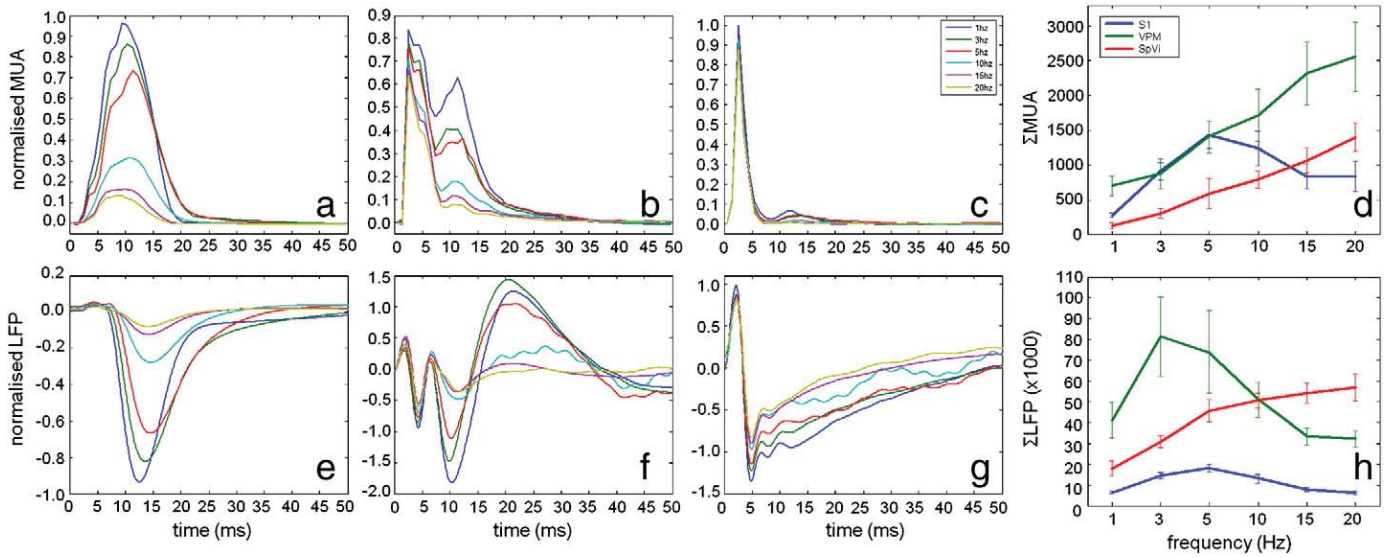

Fig. 5. Time series of LFP and MUA responses to varying stimulation frequency in the three structures of interest; these represent the average responses to each electrical pulse applied to the whisker pad over the 40 s stimulation period; a,e) S1; b,f) VPM; c,g) SpVi. In order to provide a true reflection of the overall size of neural activity, the absolute integral (Σ) of these responses were multiplied by the number of stimulus pulses in a train (e.g. 40 at 1 Hz, 800 at 20 Hz) to arrive at the integrated responses shown for MUA (d) and LFP (h). Data are average responses from all animals.

was plotted against absolute ΣMUA (Fig. 5d) and ΣLFP (Fig. 5h) responses and the ability of linear ($y = ax + c$) and non-linear ($y = ax^b + c$) models (with and without offsets) to describe the data was evaluated (Fig. 6). The particular models chosen have previously been found to describe neurovascular coupling relationships under a range of conditions (Devor et al., 2003; Hewson-Stoate et al., 2005; Norup Nielsen and Lauritzen, 2001; Sheth et al., 2004). ΣMUA and ΣLFP represent overall neural activity evoked in the 40 s duration stimulus period. Therefore, the time courses of average responses to individual electrical pulses (Fig. 5 a–c, e–g) were multiplied by the overall total number of stimuli (e.g. 40 at 1 Hz, 800 at 20 Hz). The linear and non-linear models were optimised using a least-squares algorithm and the simplest model ($y = ax$) compared to each of the more complex models using an F-test, which balances the decrease in sum-of-squares (expected from more complex models) with the increase in the number of parameters of the models, to objectively determine the neurovascular coupling relationship for each brain area electrophysiological recording parameter.

The vast majority of neurovascular coupling relationships have been obtained by the study of cortical regions (though see (Angenstein et al., 2009; Lauritzen, 2001; Lee et al., 2010)), and there is broad consensus that a positive linear relationship abounds, at least with a conservative range of stimulation parameters (Devor et al., 2003; Hewson-Stoate et al., 2005; Jones et al., 2004). Our data agree with this (Figs. 6a,b) but also extend these findings to support a linear relationship for ΣMUA not only in the cortex but in all three stations of the WTB pathway (Figs. 6a,c,e). However, when linear regression lines are compared for each dataset, the slope of the relationship in the thalamus was found to be different from both brainstem ($F = 86.03$, $p < 0.0001$) and cortex ($F = 52.02$, $p < 0.0001$). The slope of the linear relationships in brainstem and cortex were not significantly different ($F = 1.33$, $p = 0.28$). Thus, despite the presence of linear coupling between ΣBOLD and ΣMUA in each structure, the relationship that triggers vascular changes in response to spiking activity remains different. In contrast to these linear relationships, due to the plateau exhibited by ΣLFP responses in the brainstem at high frequencies (Fig. 5h), and in conjunction with a linear rise in ΣBOLD, the neurovascular coupling relationship adopted a power-law curve: small increments in neural activity produced large increases in the BOLD signal (Fig. 6f). A further exception to the positive linear rule was in the thalamus: due to strong corticothalamic feedback (Fig. 5b), the ΣLFP in the thalamus resembled that of the cortex and exhibited frequency selectivity (at 3 Hz). ΣBOLD activity increased with stimulation frequency which, in the face of falling ΣLFP responses, gave rise to a negative linear lationship between ΣLFP and the ΣBOLD signal in the thalamus (Fig. 6d).

Discussion

By using whole-brain imaging, the current study found that there are marked regional differences in BOLD fMRI activation in response to the presentation of a sensory stimulus. By comparing this regional heterogeneity with local electrophysiological recordings, we found that not all brain structures and electrophysiological measures obeyed a simple, positive linear neurovascular coupling relationship. Therefore, while supra-threshold neural activity (i.e. MUA) could always be predicted from BOLD signals in a positive linear fashion, sub-threshold (i.e. LFP) activity was only positively linearly related to the BOLD signal in the cortex; LFP responses in the brainstem and thalamus exhibited marked exceptions to this rule.

Early studies suggested that the BOLD signal could be predicted by convolving neural activity with a linear time-invariant system (Ances et al., 2000; Boynton et al., 1996; Dale and Buckner, 1997). However, not all studies have found linear relationships between direct neural recordings and haemodynamic or metabolic responses (Devor et al., 2003; Hewson-Stoate et al., 2005; Hoffmeyer et al., 2007; Jones et al., 2004; Sheth et al., 2004). Such relationships have been the focus of much research over the past fifteen years and a consensus is now emerging that, at least in the cortex, a linear relationship characterises response dynamics (Arthurs and Boniface, 2003; Arthurs et al., 2000; Brinker et al., 1999; Heeger et al., 2000; Lauritzen, 2001; Martindale et al., 2003; Nangini et al., 2008; Ngai et al., 1999; Ou et al., 2009; Rees et al., 2000; Sheth et al., 2003; Smith et al., 2002; Ureshi et al., 2004). Note, however, that important exceptions exist in the literature but these are most often found only under specific experimental conditions: non-linear relationships are often found when sensory stimuli used are of a short-duration, in which a CBF overshoot is disproportionately high compared to long-duration

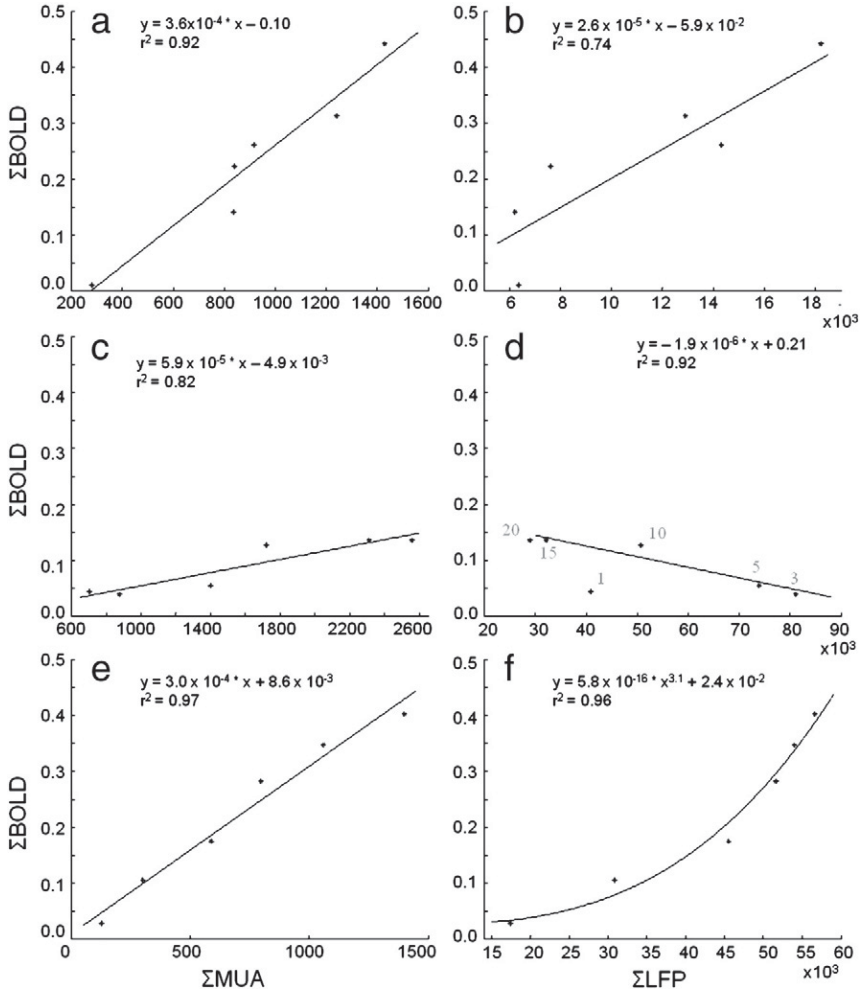

Fig. 6. Neurovascular coupling relationships. ΣLFP (a,c,e) and ΣMUA (b,d,f) responses are plotted against ΣBOLD fMRI for all three brain structures of interest and curves fitted using a least-squares model. Equations of the lines-of-fit are provided alongside R^2 values; numbers adjacent to datapoints in (d) represent stimulation frequencies. An outlier in (d), identified as the response elicited with stimulation at 1 Hz, was removed using the ROUT method (Motulsky and Brown, 2006) with a threshold of 15% prior to fitting.

stimuli (Ances et al., 2000; Soltysik et al., 2004; Vazquez and Noll, 1998) (but see (Yesilyurt et al., 2008)) or are of a low-intensity that do not cross a required neural threshold to evoke a haemodynamic response (Vazquez and Noll, 1998). In accordance with these findings, we show that neurovascular coupling in the cortex obeys a linear relationship when neural activity is triggered by long-duration sensory stimuli and modulated by altering stimulation frequency, as opposed to intensity. We also find ΣBOLD responses to be equally well predicted by ΣMUA as by ΣLFP responses in the cortex, as the absolute integral of both electrophysiological measures undergo similar, monotonic rises with increasing stimulation frequencies. Note that the cortical ΣMUA data exhibits a negative BOLD (y axis) intercept suggesting that a minimum threshold of spiking is required before a BOLD response is triggered. Excluding the ΣLFP–BOLD relationship in the thalamus (discussed below), no other structure or modality exhibits a non-zero y-intercept. This suggests that, under the experimental conditions used in the current study, neural activity in the cortex below a certain threshold would not be detected (c.f. (Zhang et al., 2008)).

The close relationship between cortical MUA and LFPs, highlighted above, is often reported in the literature (Jones et al., 2004) as is the close relationship between these measures and cortical BOLD signals (Hewson-Stoate et al., 2005; Jones et al., 2004), but there are exceptions (Logothetis et al., 2001). Poor correlations between spiking and synaptic activity can arise for a number of reasons (see below), but in the cortex a major factor is state-dependent adaptation (Kim et al., 2010). As firing thresholds are known to alter according to arousal state (McCormick and Bal, 1997), this provides a further layer of complexity to neurovascular coupling and is an issue being actively investigated (Jones et al., 2008; Masamoto et al., 2009). Such investigations, along with data from groups that have utilised unanaesthetised preparations, will play an important role in extending the results presented here to allow a comprehensive evaluation of neurovascular coupling not only across different brain regions but, crucially, between different brain states as well.

A linear relationship between ΣMUA and ΣBOLD signals was found in the brainstem, but, in contrast to the cortex, a non-linear relationship between ΣLFP responses and ΣBOLD activity was observed. A monotonic rise in ΣBOLD activity with increasing stimulus frequency (Fig. 5) suggests a lack of any threshold effect within our data. Rather, the source of the non-linearity appears to be an apparent ceiling effect of brainstem LFP responses, which, in the neurovascular relationship (Fig. 6f), resulted in small increases in ΣLFP producing proportionally larger increases in the ΣBOLD response. The non-linear coupling in the brainstem may be the result of a decrease in metabolic efficiency at high activity levels due to lower oxygen extraction fractions (Li and Freeman, 2007), which necessitate proportionately larger increases in CBF, relative to neural activity. Alternatively, the non-linearity

could result from certain components of the neural response not being accurately measured. Indeed, it is accepted that fMRI may give an account of aspects of neural activity that are undetected in conventional electrophysiological recordings (Bartels et al., 2008). For example, due to the closed-field geometry of cortically-projecting thalamic cells, components of the LFP waveform may cancel out (i.e. active sinks and passive sources could overlap (Di et al., 1990; Mitzdorf, 1985)). Furthermore, LFP recordings do not capture all aspects of synaptic activity. For instance, LFP recordings are notoriously poor at obtaining measures of inhibitory function due to the combined effect of inhibitory synapses being close to cell somata and the low amplitudes of net currents that flow during such activity (Mitzdorf, 1985). It remains unclear to what extent inhibitory synapses contribute to metabolic processes that underlie vascular responses (Enager et al., 2009; Kocharyan et al., 2008; Sotero and Trujillo-Barreto, 2007), although it is interesting that when inhibitory cell function is included in models of neurovascular coupling, non-linearities are produced (Almeida and Stetter, 2002). The extent to which synaptic inhibition explains the non-linear relationship between ΣBOLD and ΣLFP responses in the brainstem requires further investigation.

It has recently been suggested that certain brain structures may, by their very nature, not lend themselves to producing robust BOLD signals (Ekstrom, 2010). This can be due to their poor blood supply or their vasculature being relatively unreactive, either of which would result in the demand for nutrients exceeding the supply and a resultant BOLD fMRI response that is either weak, absent or negative (Ances et al., 2008; Ekstrom, 2010). In light of the present findings of weak BOLD responses in the thalamus, also reported by others (Esaki et al., 2002; Mandeville et al., 2001; Zhao et al., 2008), we suggest that this structure could fall within this category. Though capillary densities in the thalamus are similar if not greater than cortical structures (Borowsky and Collins, 1989; Gobel et al., 1990; Klein et al., 1986; Zhao and Pollack, 2009), CBF responses recorded using iodoantipyrene autoradiography (arguably a more direct measure of CBF than fMRI can provide) suggest that the vasculature is relatively unreactive as responses to sensory stimulation are approximately half the size of that in the brainstem trigeminal nuclei and barrel cortex (Esaki et al., 2002). Nonetheless, in the present study a positive linear relationship was found between ΣMUA and ΣBOLD responses in the thalamus and a negative linear relationship between ΣLFP and ΣBOLD responses. Note that despite a positive linear relationship between ΣMUA and ΣBOLD, the slope of the line was relatively shallow, and significantly different to that in the brainstem and cortex owing to the relatively weak thalamic BOLD responses. Hence, and of crucial importance, similar increases in neural activity in the three regions would give rise to dissimilar increases in BOLD.

The negative slope of the neurovascular relationship between ΣLFP and the ΣBOLD response in the thalamus is in stark contrast to the positive slope of the ΣMUA and ΣBOLD relationship (in the thalamus as well as in brainstem and cortex). The dissociation between sub-threshold (LFP) and supra-threshold (MUA) thalamic activity that underlies this difference could arise for many reasons (see above). Here the rather unusual phenomenon of an increase in MUA activity and a simultaneous decrease in LFP responses could reflect the fact that some features of neural activity are insufficiently captured by LFP recording techniques, as was mentioned above regarding the brainstem. Alternatively, lower levels of synaptic activity may be required to elicit spikes at high frequency, due for example to the effects of temporal summation. Accordingly, the single ΣLFP–ΣBOLD data point in Fig. 6d that has been identified as an outlier is that from the 1 Hz stimulation frequency and, we suggest lies outside the linear relationship because neural activity elicited was insufficient to bring about a haemodynamic response. Regardless of the cause of the negative ΣLFP–ΣBOLD relationship in the thalamus, the fact that the BOLD responses in the thalamus (and trigeminal nucleus) are better predicted by MUA than by LFP lends support to the argument that spiking activity is more closely related to the BOLD response, and the associated haemodynamic and metabolic processes (Heeger et al., 2000; Masino, 2003; Mukamel et al., 2005; Smith et al., 2002). However, for the reasons discussed above, this may not be a result of greater energy requirements of spiking activity as some groups suggest (Heeger and Ress, 2002; Nir et al., 2008).

Conclusions

In any study of neurovascular coupling, one must ask how the data obtained may be applied to enable better understanding and interpretation of imaging signals. To this end, the widely-held consensus of a simple, positive linear relationship existing between neural activity and BOLD signals in the cerebral cortex has facilitated the widespread application of fMRI in studies of cognition that are, by definition, centred on cortical function. The current findings of dissimilar relationships in non-cortical structures need not limit the application of fMRI to studies in which such regions are the focus but do recommend a 'proceed with caution' approach for cognitive neuroscientists investigating the function of non-cortical brain regions, especially when comparing them to cortical regions. Our study also strongly argues for further investigations to be made into the true origins of the BOLD signal in different brain regions not only in anaesthetised (or even awake) subjects at rest but also during different states of arousal, a related discipline that has as many controversies as the study of neurovascular coupling (Arthurs et al., 2004; Jones et al., 2008; Sirotin and Das, 2009). Clearly there is still much work to do before all the information hidden within fMRI signals is decoded.

Acknowledgments

This work was funded by a Biotechnology and Biological Sciences Research Council grant (BBE0073761). We are grateful to the technical assistance provided by Dr David Johnston, Marion Simkins and Natalie Kennerley.

References

Almeida, R., Stetter, M., 2002. Modeling the link between functional imaging and neuronal activity: synaptic metabolic demand and spike rates. Neuroimage 17, 1065–1079.
Ances, B.M., Zarahn, E., Greenberg, J.H., Detre, J.A., 2000. Coupling of neural activation to blood flow in the somatosensory cortex of rats is time-intensity separable, but not linear. J. Cereb. Blood Flow Metab. 20, 921–930.
Ances, B.M., Leontiev, O., Perthen, J.E., Liang, C., Lansing, A.E., Buxton, R.B., 2008. Regional differences in the coupling of cerebral blood flow and oxygen metabolism changes in response to activation: implications for BOLD-fMRI. Neuroimage 39, 1510–1521.
Angenstein, F., Kammerer, E., Scheich, H., 2009. The BOLD response in the rat hippocampus depends rather on local processing of signals than on the input or output activity. A combined functional MRI and electrophysiological study. J. Neurosci. 29, 2428–2439.
Arthurs, O.J., Boniface, S.J., 2003. What aspect of the fMRI BOLD signal best reflects the underlying electrophysiology in human somatosensory cortex? Clin. Neurophysiol. 114, 1203–1209.
Arthurs, O.J., Williams, E.J., Carpenter, T.A., Pickard, J.D., Boniface, S.J., 2000. Linear coupling between functional magnetic resonance imaging and evoked potential amplitude in human somatosensory cortex. Neuroscience 101, 803–806.
Arthurs, O.J., Johansen-Berg, H., Matthews, P.M., Boniface, S.J., 2004. Attention differentially modulates the coupling of fMRI BOLD and evoked potential signal amplitudes in the human somatosensory cortex. Exp. Brain Res. 157, 269–274.
Bartels, A., Logothetis, N.K., Moutoussis, K., 2008. fMRI and its interpretations: an illustration on directional selectivity in area V5/MT. Trends Neurosci. 31, 444–453.
Boorman, L., Kennerley, A.J., Johnston, D., Jones, M., Zheng, Y., Redgrave, P., Berwick, J., 2010. Negative blood oxygen level dependence in the rat: a model for investigating the role of suppression in neurovascular coupling. J. Neurosci. 30, 4285–4294.
Borowsky, I.W., Collins, R.C., 1989. Metabolic anatomy of brain: a comparison of regional capillary density, glucose metabolism, and enzyme activities. J. Comp. Neurol. 288, 401–413.
Boynton, G.M., Engel, S.A., Glover, G.H., Heeger, D.J., 1996. Linear systems analysis of functional magnetic resonance imaging in human V1. J. Neurosci. 16, 4207–4221.
Brinker, G., Bock, C., Busch, E., Krep, H., Hossmann, K.A., Hoehn-Berlage, M., 1999. Simultaneous recording of evoked potentials and T2*-weighted MR images during somatosensory stimulation of rat. Magn. Reson. Med. 41, 469–473.

Brozoski, T.J., Caspary, D.M., Bauer, C.A., 2006. Marking multi-channel silicon-substrate electrode recording sites using radiofrequency lesions. J. Neurosci. Methods 150, 185–191.
Cavaglia, M., Dombrowski, S.M., Drazba, J., Vasanji, A., Bokesch, P.M., Janigro, D., 2001. Regional variation in brain capillary density and vascular response to ischemia. Brain Res. 910, 81–93.
Chiarelli, P.A., Bulte, D.P., Gallichan, D., Piechnik, S.K., Wise, R., Jezzard, P., 2007. Flow-metabolism coupling in human visual, motor, and supplementary motor areas assessed by magnetic resonance imaging. Magn. Reson. Med. 57, 538–547.
Cholet, N., Seylaz, J., Lacombe, P., Bonvento, G., 1997. Local uncoupling of the cerebrovascular and metabolic responses to somatosensory stimulation after neuronal nitric oxide synthase inhibition. J. Cereb. Blood Flow Metab. 17, 1191–1201.
Dale, A.M., Buckner, R.L., 1997. Selective averaging of rapidly presented individual trials using fMRI. Hum. Brain Mapp. 5, 329–340.
Detre, J.A., Ances, B.M., Takahashi, K., Greenberg, J.H., 1998. Signal averaged laser Doppler measurements of activation-flow coupling in the rat forepaw somatosensory cortex. Brain Res. 796, 91–98.
Devonshire, I.M., Berwick, J., Jones, M., Martindale, J., Johnston, D., Overton, P.G., Mayhew, J.E., 2004. Haemodynamic responses to sensory stimulation are enhanced following acute cocaine administration. Neuroimage 22, 1744–1753.
Devor, A., Dunn, A.K., Andermann, M.L., Ulbert, I., Boas, D.A., Dale, A.M., 2003. Coupling of total hemoglobin concentration, oxygenation, and neural activity in rat somatosensory cortex. Neuron 39, 353–359.
Di, S., Baumgartner, C., Barth, D.S., 1990. Laminar analysis of extracellular field potentials in rat vibrissa/barrel cortex. J. Neurophysiol. 63, 832–840.
Diamond, M.E., Armstrong-James, M., Ebner, F.F., 1992. Somatic sensory responses in the rostral sector of the posterior group (POm) and in the ventral posterior medial nucleus (VPM) of the rat thalamus. J. Comp. Neurol. 318, 462–476.
Duvernoy, H.M., Delon, S., Vannson, J.L., 1981. Cortical blood vessels of the human brain. Brain Res. Bull. 7, 519–579.
Ekstrom, A., 2010. How and when the fMRI BOLD signal relates to underlying neural activity: the danger in dissociation. Brain Res. Rev. 62, 233–244.
Enager, P., Piilgaard, H., Offenhauser, N., Kocharyan, A., Fernandes, P., Hamel, E., Lauritzen, M., 2009. Pathway-specific variations in neurovascular and neurometabolic coupling in rat primary somatosensory cortex. J. Cereb. Blood Flow Metab. 29, 976–986.
Esaki, T., Itoh, Y., Shimoji, K., Cook, M., Jehle, J., Sokoloff, L., 2002. Effects of dopamine receptor blockade on cerebral blood flow response to somatosensory stimulation in the unanesthetized rat. J. Pharmacol. Exp. Ther. 303, 497–502.
Fraser, G., Hartings, J.A., Simons, D.J., 2006. Adaptation of trigeminal ganglion cells to periodic whisker deflections. Somatosens. Mot. Res. 23, 111–118.
Frostig, R.D., 2006. Functional organization and plasticity in the adult rat barrel cortex: moving out-of-the-box. Curr. Opin. Neurobiol. 16, 445–450.
Gobel, U., Theilen, H., Kuschinsky, W., 1990. Congruence of total and perfused capillary network in rat brains. Circ. Res. 66, 271–281.
Gotoh, J., Kuang, T.Y., Nakao, Y., Cohen, D.M., Melzer, P., Itoh, Y., Pak, H., Pettigrew, K., Sokoloff, L., 2001. Regional differences in mechanisms of cerebral circulatory response to neuronal activation. Am. J. Physiol. Heart Circ. Physiol. 280, H821–H829.
Heeger, D.J., Ress, D., 2002. What does fMRI tell us about neuronal activity? Nat. Rev. Neurosci. 3, 142–151.
Heeger, D.J., Huk, A.C., Geisler, W.S., Albrecht, D.G., 2000. Spikes versus BOLD: what does neuroimaging tell us about neuronal activity? Nat. Neurosci. 3, 631–633.
Hewson-Stoate, N., Jones, M., Martindale, J., Berwick, J., Mayhew, J., 2005. Further nonlinearities in neurovascular coupling in rodent barrel cortex. Neuroimage 24, 565–574.
Hoffmeyer, H.W., Enager, P., Thomsen, K.J., Lauritzen, M.J., 2007. Nonlinear neurovascular coupling in rat sensory cortex by activation of transcallosal fibers. J. Cereb. Blood Flow Metab. 27, 575–587.
Huettel, S.A., McKeown, M.J., Song, A.W., Hart, S., Spencer, D.D., Allison, T., McCarthy, G., 2004. Linking hemodynamic and electrophysiological measures of brain activity: evidence from functional MRI and intracranial field potentials. Cereb. Cortex 14, 165–173.
Jones, M., Berwick, J., Johnston, D., Mayhew, J., 2001. Concurrent optical imaging spectroscopy and laser-Doppler flowmetry: the relationship between blood flow, oxygenation, and volume in rodent barrel cortex. Neuroimage 13, 1002–1015.
Jones, M., Hewson-Stoate, N., Martindale, J., Redgrave, P., Mayhew, J., 2004. Nonlinear coupling of neural activity and CBF in rodent barrel cortex. Neuroimage 22, 956–965.
Jones, M., Devonshire, I.M., Berwick, J., Martin, C., Redgrave, P., Mayhew, J., 2008. Altered neurovascular coupling during information-processing states. Eur. J. Neurosci. 27, 2758–2772.
Keilholz, S.D., Silva, A.C., Raman, M., Merkle, H., Koretsky, A.P., 2004. Functional MRI of the rodent somatosensory pathway using multislice echo planar imaging. Magn. Reson. Med. 52, 89–99.
Khatri, V., Hartings, J.A., Simons, D.J., 2004. Adaptation in thalamic barreloid and cortical barrel neurons to periodic whisker deflections varying in frequency and velocity. J. Neurophysiol. 92, 3244–3254.
Kim, T., Masamoto, K., Fukuda, M., Vazquez, A., Kim, S.G., 2010. Frequency-dependent neural activity, CBF, and BOLD fMRI to somatosensory stimuli in isoflurane-anesthetized rats. Neuroimage 52, 224–233.
Klein, B., Kuschinsky, W., Schrock, H., Vetterlein, F., 1986. Interdependency of local capillary density, blood flow, and metabolism in rat brains. Am. J. Physiol. 251, H1333–H1340.
Kocharyan, A., Fernandes, P., Tong, X.K., Vaucher, E., Hamel, E., 2008. Specific subtypes of cortical GABA interneurons contribute to the neurovascular coupling response to basal forebrain stimulation. J. Cereb. Blood Flow Metab. 28, 221–231.
Lauritzen, M., 2001. Relationship of spikes, synaptic activity, and local changes of cerebral blood flow. J. Cereb. Blood Flow Metab. 21, 1367–1383.
Lauritzen, M., Gold, L., 2003. Brain function and neurophysiological correlates of signals used in functional neuroimaging. J. Neurosci. 23, 3972–3980.
Lee, J.H., Durand, R., Gradinaru, V., Zhang, F., Goshen, I., Kim, D.S., Fenno, L.E., Ramakrishnan, C., Deisseroth, K., 2010. Global and local fMRI signals driven by neurons defined optogenetically by type and wiring. Nature 465, 788–792.
Li, B., Freeman, R.D., 2007. High-resolution neurometabolic coupling in the lateral geniculate nucleus. J. Neurosci. 27, 10223–10229.
Logothetis, N.K., Wandell, B.A., 2004. Interpreting the BOLD signal. Annu. Rev. Physiol. 66, 735–769.
Logothetis, N.K., Pauls, J., Augath, M., Trinath, T., Oeltermann, A., 2001. Neurophysiological investigation of the basis of the fMRI signal. Nature 412, 150–157.
Mandeville, J.B., Jenkins, B.G., Kosofsky, B.E., Moskowitz, M.A., Rosen, B.R., Marota, J.J., 2001. Regional sensitivity and coupling of BOLD and CBV changes during stimulation of rat brain. Magn. Reson. Med. 45, 443–447.
Martindale, J., Mayhew, J., Berwick, J., Jones, M., Martin, C., Johnston, D., Redgrave, P., Zheng, Y., 2003. The hemodynamic impulse response to a single neural event. J. Cereb. Blood Flow Metab. 23, 546–555.
Martuzzi, R., Murray, M.M., Meuli, R.A., Thiran, J.P., Maeder, P.P., Michel, C.M., de Peralta, Grave, Menendez, R., Gonzalez Andino, S.L., 2009. Methods for determining frequency- and region-dependent relationships between estimated LFPs and BOLD responses in humans. J. Neurophysiol. 101, 491–502.
Masamoto, K., Fukuda, M., Vazquez, A., Kim, S.G., 2009. Dose-dependent effect of isoflurane on neurovascular coupling in rat cerebral cortex. Eur. J. Neurosci. 30, 242–250.
Masino, S.A., 2003. Quantitative comparison between functional imaging and single-unit spiking in rat somatosensory cortex. J. Neurophysiol. 89, 1702–1712.
McCormick, D.A., Bal, T., 1997. Sleep and arousal: thalamocortical mechanisms. Annu. Rev. Neurosci. 20, 185–215.
Minnery, B.S., Simons, D.J., 2003. Response properties of whisker-associated trigeminothalamic neurons in rat nucleus principalis. J. Neurophysiol. 89, 40–56.
Mitzdorf, U., 1985. Current source-density method and application in cat cerebral cortex: investigation of evoked potentials and EEG phenomena. Physiol. Rev. 65, 37–100.
Moonen, C.T.W., Bandettini, P.A. (Eds.), 2000. Functional MRI. Springer.
Moreno, A., Garcia-Gonzalez, V., Sanchez-Jimenez, A., Panetsos, F., 2005. Principalis, oralis and interpolaris responses to whisker movements provoked by air jets in rats. Neuroreport 16, 1569–1573.
Motulsky, H.J., Brown, R.E., 2006. Detecting outliers when fitting data with nonlinear regression — a new method based on robust nonlinear regression and the false discovery rate. BMC Bioinformatics 7, 123.
Mukamel, R., Gelbard, H., Arieli, A., Hasson, U., Fried, I., Malach, R., 2005. Coupling between neuronal firing, field potentials, and FMRI in human auditory cortex. Science 309, 951–954.
Nangini, C., Tam, F., Graham, S.J., 2008. A novel method for integrating MEG and BOLD fMRI signals with the linear convolution model in human primary somatosensory cortex. Hum. Brain Mapp. 29, 97–106.
Ngai, A.C., Jolley, M.A., D'Ambrosio, R., Meno, J.R., Winn, H.R., 1999. Frequency-dependent changes in cerebral blood flow and evoked potentials during somatosensory stimulation in the rat. Brain Res. 837, 221–228.
Nir, Y., Dinstein, I., Malach, R., Heeger, D.J., 2008. BOLD and spiking activity. Nat. Neurosci. 11, 523–524 (author reply 524).
Norup Nielsen, A., Lauritzen, M., 2001. Coupling and uncoupling of activity-dependent increases of neuronal activity and blood flow in rat somatosensory cortex. J. Physiol. 533, 773–785.
Ou, W., Nissila, I., Radhakrishnan, H., Boas, D.A., Hamalainen, M.S., Franceschini, M.A., 2009. Study of neurovascular coupling in humans via simultaneous magnetoencephalography and diffuse optical imaging acquisition. Neuroimage 46, 624–632.
Paxinos, G., Watson, C., 1998. The Rat Brain in Stereotaxic Coordinates. Academic Press.
Petersen, C.C., 2007. The functional organization of the barrel cortex. Neuron 56, 339–355.
Rees, G., Friston, K., Koch, C., 2000. A direct quantitative relationship between the functional properties of human and macaque V5. Nat. Neurosci. 3, 716–723.
Rieke, G.K., 1987. Thalamic arterial pattern: an endocast and scanning electron microscopic study in normotensive male rats. Am. J. Anat. 178, 45–54.
Sheth, S., Nemoto, M., Guiou, M., Walker, M., Pouratian, N., Toga, A.W., 2003. Evaluation of coupling between optical intrinsic signals and neuronal activity in rat somatosensory cortex. Neuroimage 19, 884–894.
Sheth, S.A., Nemoto, M., Guiou, M., Walker, M., Pouratian, N., Toga, A.W., 2004. Linear and nonlinear relationships between neuronal activity, oxygen metabolism, and hemodynamic responses. Neuron 42, 347–355.
Sheth, S.A., Nemoto, M., Guiou, M.W., Walker, M.A., Toga, A.W., 2005. Spatiotemporal evolution of functional hemodynamic changes and their relationship to neuronal activity. J. Cereb. Blood Flow Metab. 25, 830–841.
Shoykhet, M., Doherty, D., Simons, D.J., 2000. Coding of deflection velocity and amplitude by whisker primary afferent neurons: implications for higher level processing. Somatosens. Mot. Res. 17, 171–180.
Sigalovsky, I.S., Melcher, J.R., 2006. Effects of sound level on fMRI activation in human brainstem, thalamic and cortical centers. Hear. Res. 215, 67–76.
Sirotin, Y.B., Das, A., 2009. Anticipatory haemodynamic signals in sensory cortex not predicted by local neuronal activity. Nature 457, 475–479.
Smith, A.J., Blumenfeld, H., Behar, K.L., Rothman, D.L., Shulman, R.G., Hyder, F., 2002. Cerebral energetics and spiking frequency: the neurophysiological basis of fMRI. Proc. Natl. Acad. Sci. U.S.A. 99, 10765–10770.
Soltysik, D.A., Peck, K.K., White, K.D., Crosson, B., Briggs, R.W., 2004. Comparison of hemodynamic response nonlinearity across primary cortical areas. Neuroimage 22, 1117–1127.

Sosnik, R., Haidarliu, S., Ahissar, E., 2001. Temporal frequency of whisker movement. I. Representations in brain stem and thalamus. J. Neurophysiol. 86, 339–353.
Sotero, R.C., Trujillo-Barreto, N.J., 2007. Modelling the role of excitatory and inhibitory neuronal activity in the generation of the BOLD signal. Neuroimage 35, 149–165.
Spenger, C., Josephson, A., Klason, T., Hoehn, M., Schwindt, W., Ingvar, M., Olson, L., 2000. Functional MRI at 4.7 Tesla of the rat brain during electric stimulation of forepaw, hindpaw, or tail in single- and multislice experiments. Exp. Neurol. 166, 246–253.
Stewart Jr., D.H., King, R.B., 1966. Effect of conditioning stimuli upon evoked potentials in the trigeminal complex. J. Neurophysiol. 29, 442–455.
Temereanca, S., Simons, D.J., 2003. Local field potentials and the encoding of whisker deflections by population firing synchrony in thalamic barreloids. J. Neurophysiol. 89, 2137–2145.
Tuunanen, P.I., Murray, I.J., Parry, N.R., Kauppinen, R.A., 2006. Heterogeneous oxygen extraction in the visual cortex during activation in mild hypoxic hypoxia revealed by quantitative functional magnetic resonance imaging. J. Cereb. Blood Flow Metab. 26, 263–273.
Ureshi, M., Matsuura, T., Kanno, I., 2004. Stimulus frequency dependence of the linear relationship between local cerebral blood flow and field potential evoked by activation of rat somatosensory cortex. Neurosci. Res. 48, 147–153.
Vafaee, M.S., Gjedde, A., 2004. Spatially dissociated flow-metabolism coupling in brain activation. Neuroimage 21, 507–515.
Vazquez, A.L., Noll, D.C., 1998. Nonlinear aspects of the BOLD response in functional MRI. Neuroimage 7, 108–118.
Yesilyurt, B., Ugurbil, K., Uludag, K., 2008. Dynamics and nonlinearities of the BOLD response at very short stimulus durations. Magn. Reson. Imaging 26, 853–862.
Yu, X., Wadghiri, Y.Z., Sanes, D.H., Turnbull, D.H., 2005. In vivo auditory brain mapping in mice with Mn-enhanced MRI. Nat. Neurosci. 8, 961–968.
Zhang, N., Liu, Z., He, B., Chen, W., 2008. Noninvasive study of neurovascular coupling during graded neuronal suppression. J. Cereb. Blood Flow Metab. 28, 280–290.
Zhao, R., Pollack, G.M., 2009. Regional differences in capillary density, perfusion rate, and P-glycoprotein activity: a quantitative analysis of regional drug exposure in the brain. Biochem. Pharmacol. 78, 1052–1059.
Zhao, F., Zhao, T., Zhou, L., Wu, Q., Hu, X., 2008. BOLD study of stimulation-induced neural activity and resting-state connectivity in medetomidine-sedated rat. Neuroimage 39, 248–260.
Zheng, Y., Johnston, D., Berwick, J., Mayhew, J., 2001. Signal source separation in the analysis of neural activity in brain. Neuroimage 13, 447–458.